PROCEEDINGS, Thirty-Sixth Workshop on Geothermal Reservoir Engineering
Stanford University, Stanford, California, January 31 - February 2, 2011
SGP-TR-191

Induced Stress in a Geothermal Doublet System

A. Hassanzadegan, G. Blöcher, G. Zimmermann, H. Milsch, I. Moeck
Helmholtz Centre Potsdam - GFZ German Research Centre for Geosciences,
Telegrafenberg
Potsdam, Brandenburg, D-1447, Germany
e-mail: alireza.hassanzadegan@gfz-potsdam.de

ABSTRACT

This paper presents the predicted magnitudes of induced thermoelastic and poroelastic stresses and the resulting reservoir deformation, caused by production and injection of water into Groß Schönebeck geothermal Reservoir. The Groß Schönebeck reservoir is a confined aquifer, located at about 4 km depth within the Lower Permian of the North East German Basin. The geological formation is composed from bottom to top of volcanic and siliciclastic rocks. Injection of cold water into a hot water reservoir will contract the rock, however the surrounding rock will constrain this contraction and thermal stress will be induced. This thermally induced stress not only influences the rock mechanical properties but also affects the poroelastic and consequently transport properties of the rock. While geomechanics in conventional reservoir simulator is often governed by change in pore compressibility and permeability as a function of pressure, a coupled mechanical and fluid flow simulator attempts to capture the alterations in reservoir properties (mainly porosity and permeability) due to changes in pressure, temperature and the induced stress and deformation.

In order to predict the thermal effects in reservoir scale, a static model which includes reservoir structure (geological units, faults and induced hydraulic fractures) was created. Thermo-hydro-mechanical analysis of the reservoir was performed for 30 years, the expected life cycle of the reservoir. A transition stress regime between normal faulting to strike-slip faulting is expected in Groß Schönebeck geothermal reservoir; hence different boundary conditions are employed. In particular, porosity and permeability were coupled through the changes in the strain and stress. The induced thermoelastic stress makes the minimum horizontal stress more tensile and pore pressure controls the effective stress. Fracturing would occur if the minimum principal effective stress becomes tensile and equal to tensile strength of the rock. A temperature decrease of 80 °C and an increase of 10 MPa in bottomhole pressure due to water injection, results in a change in minimum horizontal effective stress, such that it exceeds the tensile strength (3.9 MPa) of the rock.

INTRODUCTION

This paper addresses the modelling of the geomechanical effects induced by reservoir production and reinjection and their influence on hydrothermal processes occurring in an enhanced geothermal system (EGS) during geothermal power production. While reservoir enginering attempts to provide answers on the extent of the reservoirs, the optimum production rate and the reservoir performance, reservoir geomechanics tries to capture rock-fluid interaction in terms of the stress and deformation and to characterize the failure of the rock. Geomechanical response may have a strong effect on the productiivity and injectivity response of the reservoir. Due to pore pressure and temperature changes, the in situ stress will change and rock will deform. Coupling of deformation and pore pressure diffusion (Darcy's law) characterizes the mechanical response of fluid-saturated porous rocks. Thermal stress may arise in a heated body either because of a non-uniform temperature distribution or external boundaries or a combination of both.

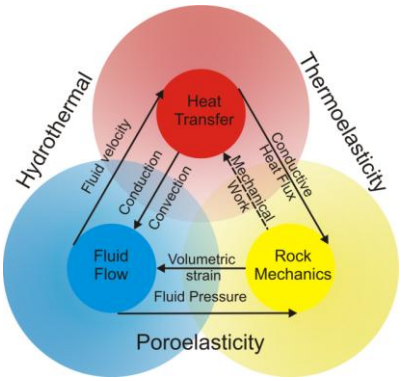

Figure 1 : Thermo-Hydro-Mechanical processes. Each process affects the initiation and progress of the other one.

A 30 years water cycling between production well and injection well was modelled using a 3D stress dependent reservoir simulator (RGCoE, 2010). The special focus will be on the modelling of the stress and displacement evolution during reservoir life cycle.

Geomechanical effects

In a doublet well system the in situ stress changes due to production and reinjection of cold water. Pore pressure alters the effective stresses acting on the rock. Two basic mechanics highlights poroelastic coupling : first, increase in pore pressure will dilate the rock and second a rapid loading or compression will increase the pressure in trapped fluid (undrained conditions). In drained conditions the pore presure is dissipitated according to the diffusion law. Furthermore, a pore pressure gradient results in seepage forces at steady state fluid flow. Seepage forces induce stresses within the porous body that should be take into account in the equilibrium of the effective stresses (Detournay & Cheng, 1988). It is the effective stress which control both compressive and tensile failure. If the strains are high enough, the rock fails either in shear or in tension. Three stress regimes can be defined if the rock fails in shear: Normal fault regime, strike slip fault and thrust (reverse) fault (Fjaer, Holt, Horsrud, & Raaen, 1992). Segall and Fitzgerald (1998) investigated stress changes in hydrocarbon and geothermal reservoirs. According to this study, thermal stresses may exceed poroelastic stresses by a factor of 8 or more. This indicates that thermoelastic behavior of rock cannot be ignored. Stress changes within the reservoir can be calculated if the appropriate hydraulic and poroelastic parameters are known.The following equation can be employed to quantify the ratio between thermoelastic (σ_T) and poroelastic (σ_p) stresses due to injection and production in geothermal reservoirs:

1

$$\frac{\sigma_T}{\sigma_p} = \frac{3\beta\Delta T}{\alpha\Delta p/K}$$

where α is Biot's coefficient K is the bulk modulus, β is the linear thermal expansion coefficient and ΔT and ΔP are the change in temperature and pressure respectively. Uniaxial deformation assumption (sides and bottom of reservoir constrained) has been one of the most popular approaches to model the geomechanical behaviour of reservoirs. Assuming uniaxial boundary conditions where no horizontal strain occurs the ratio of changes in horizontal stress due to changes in reservoir pressure and temperature can be estimated.

2

$$\frac{\Delta S_h}{\Delta P} = -\frac{1-2\nu}{1-\nu}\alpha$$

where S_h is the minimum horizontal stress, ν is the Poisson's ratio and the right hand side is equal to poroelastic stress coefficient. Thermoelastic stress and strain evolution due to temperature variations in uniaxial boundary conditions can be estimated according to the following equation:

3

$$\sigma_T = \frac{E\beta\Delta T}{1-\nu}$$

where E is the Young's modulus and $\boldsymbol{E\beta/(1-\nu)}$ is the thermoelastic stress coefficient.

4

$$\varepsilon_v = \frac{1+\nu}{1-\nu}\,\beta\Delta T$$

An increase in temperature causes an increase in volume and results in compressional thermoelastic stress. A decrease in temperature causes a reduction in volume and results in tensile stresses. Thermoelastic effects predominates in case of increase in rock mechanical stiffness, which could be due to an increase in confining pressure. The Biot effective coefficient is defined as the contribution of pore pressure to the total stress, i.e. the efficiency of pore fluid in counteracting to the total applied stress.

5

$$\sigma^{eff} = \sigma + \alpha P_p$$

Rock will fail in tensile mode if the minimum effective principal stress becomes tensile and equal to the tensile strength of the rock (Fjaer, Holt, Horsrud, & Raaen, 1992):

6

$$\sigma_3^{\mathrm{eff}} = \sigma_3 + \alpha P_p \geq \sigma_{\mathrm{tensile}}$$

Groß Schönebeck-Geothermal Reservoir

The Groß Schönebeck geothermal reservoir is a research site in the North German Basin. The technical feasibility of geothermal power production from a deep low-enthalpy reservoir will be evaluated by means of a doublet system consisting of a production and injection well. The research strategy and challenges while drilling the wells have already being discussed in previous works: Legarth, Huenges, & Zimmermann (2005), Huenges, et al., (2007) and Kwiatek, et al. (2008).

An existing gas exploration well (GrSk3) was reopened and deepened up to a depth of approximately 4,300 m. Several hydraulic stimulations have been carried out in this well to serve as an injection well (Legarth, Huenges, & Zimmermann, 2005). A deviated production well

(GrSk4) has been drilled in the direction of minimum horizontal stress. Both wells are placed in one drilling site at a distance of 28 meters at surface. At the top of the reservoir the wells have a distance of 241 m. This distance is increasing to 470 meters by increasing the inclination of production well progressively from 18° to 48°. Three stimulation treatments have been performed to enhance the productivity of the production well. The induced hydraulic fractures have been propagating perpendicular to the well path (Zimmermann, et al., 2007).The Groß Schönebeck reservoir is a faulted reservoir. The reservoir is located at a depth of 3700 to 4300 m subsea. The fault pattern was interpretated by 2D seismic data. The trend of major fault is N-W and minor faults are characterized by a NE-N direction.

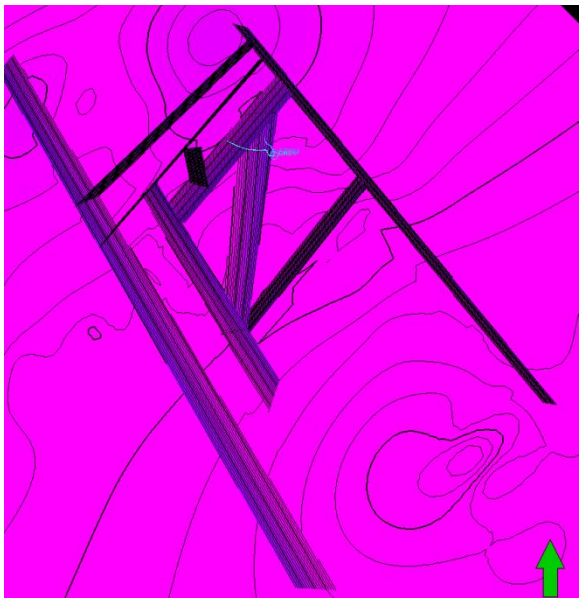

Figure 2: Top view of the fault pattern. Major faults have a trend of NW and minor faults have a trend of NE-N.

Reservoir geology

The reservoir formation consists of two different rock types: sedimentary sandstones and volcanic rocks. Lower Permian siliciclastic sediments and volcanic are widespread strata throughout Central Europe forming deeply buried aquifers in the North German Basin with formation temperatures of up to 150°C. The average depth of these strata is 4000 m. The main reservoir interval is the sandstones of the Upper Rotliegend (Dethlingen Formation). A shale cap rock covers the reservoir. Underneath, the Hannover formation is placed which has a high concentration of silts and mudstones. The Dethlingen formation consists of three sub layers: (1) Elbe alternating sequence, mostly consists of silt to fine grained sandstone. (2) Elbe base sandstone- II composed of fine grained sandstone (3) Elbe base sandstone -I, consists of fine to middle grained sandstone. The Havel formation is the most lowest sedimentary geological unit, consisting of mainly conglomerates. Beneath the sedimentary strata, a volcanic formation is placed.

Initial condition

The pore pressure is determined by production logs at stationary condition to be 43.8 MPa at a depth of 4220 mss (Legarth, Huenges, & Zimmermann, 2005). The reservoir fluid is saline water with a density of 1109 kg/m^3. The gas phase is dominated by N2 (80 vol. %) and CH4 (15 vol. %) which is typical for the natural gas composition found in the Rotliegend sandstones. The gas-water volume ratio in the sampled fluids was approximately 1 at ambient conditions. The temperature gradient in the reservoir is such that the Hannover formation has a temperature of 138°C and temperature increases continuously to 147°C for the volcanic rocks.

In situ stress state

The in situ stress state was determined for this Lower Permian (Rotliegend) reservoir by an integrated approach of 3D structural modelling, 3D fault mapping and stress ratio definition based on frictional constraints, and slip-tendency analysis (Moeck, Schandelmeier, & Holl, 2008).
The azimuth of the maximum horizontal stress was obtained by analysing the acoustic borehole televiewer (ABF14) images and formation microimages (FMI) to be 18.5±3.7° (Holl, et al., 2003). The minimum horizontal stress (S_h) magnitude is evaluated by hydraulic fracturing to be 54 MPa. The vertical stress (S_v) was estimated by considering the average weight of the overburden strata and the thickness of the rock units. An equivalent density of 2500 kg/m^3 for the entire overburden was calculated. Consequently, vertical stress is equal to 100 MPa at a depth of 4100 meter. The most uncertain component of stress tensor is maximum horizontal stress (S_H). Jaeger et al. (2007) derived the ratio between effective principal stresses as a function of sliding friction coefficient, which can be employed to give the bounds on S_H. Moeck et al., (2008) employed this approach and stated that the maximum horizontal stress is equal or less than 0.78 S_v in normal faulting regime. In strike slip faulting regime it is equal or less than vertical stress S_v. A value of 95-100 MPa is confirmed by core tests and numerical modelling. Therefore, the stationary effective mean stress can be calculated by:

7

$$\sigma_m^{eff} = \frac{1}{3}(S_V + S_h + S_H) - P_p$$

to be 40.4 MPa. The effective Terzaghi stress is defined as $S_{eff}= S-P_p$, where P_p is pore pressure and S is a component of principal stress tensor.

The NE-trending faults carry the highest ratio of shear to normal stresses. These faults exhibit a critically stress state in the sandstones and a highly stressed state in the volcanic layer. Since critically stressed faults are described as hydraulically conductive (Barton, Zoback, & Moos, 1995) these NE-N trending faults are expected to be the main fluid pathways in the reservoir (Moeck, Schandelmeier, & Holl, 2008). During the hydraulic fracturing of production well microseismicity was monitored by a three-axis geophone, installed in the injection well (GrSk3) at a depth of 3735 m. The orientation of the seismic events is approximately in the north-south direction and hence similar to the maximum horizontal stress direction (Kwiatek, et al., 2008)

MODELING

There are different approaches to analyse the geomechanical effects in a geothermal reservoir, categorized as analytical models, semi-analytical models and numerical models. Semi-analytical models are those which use analytical solutions including numerical integration procedures. Segall and Fitzgerald (1998) studied simple geometric reservoirs by employing semi analytical solutions to evaluate stress changes both within a reservoir and in the surrounding rocks. To analyze more complicated reservoirs, accounting for more realistic geometries and rock/fluid behavior, the use of numerical models is required. Moeck, et al., (2008) provided a 3D regional model which includes the surface horizons, fault geometries and well trajectories. Bloecher, et al., (2010) studied the coupling between hydrothermal processes by employing a finite element simulation. They have captured the structure of the reservoir using unstructured grids consisting of triangular prisms. His model captures the coupling of various petrophysical parameters and it includes pressure and temperature dependency of the heat conductivity, heat capacity, fluid density and viscosity. In this paper the corner point grid geometries capture the reservoir structure as it is convenient in many reservoir simulators. In order to construct the static model, horizon surfaces, well trajectories, faults and hydraulic induced fractures were implemented into the Flogrid-Petrel software and reservoir structure was captured. The faults are described using directional transmissibility multipliers for the fluid flow problem. The reservoir model was based on a single porosity description for fluid flow. The hydrothermal modelling was performed by employing Eclipse™ software (GeoQuest, 2010). The Thermo-hydro-mechanical (THM) modelling was performed by employing Visage™ (RGCoE, 2010).

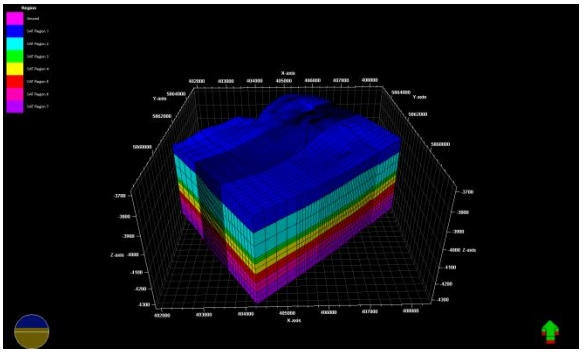

Figure 3: Reservoir structure build in Petrel. The boundary of models following the northwest major faults.

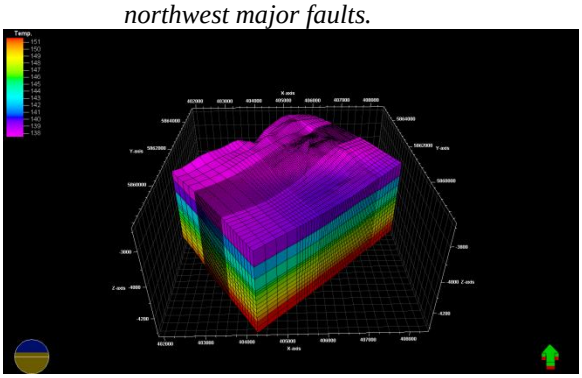

Figure 4: Reservoir temperature varies between 137ºC at the cap rock to 151ºC, at bottom hole.

Input parameters

In thermo-hydro-mechanical modelling different processes are involved and therefore different kind of material properties are required to characterize the reservoir. These properties can be categorized to hydraulical, thermal and mechanical properties.

Thermo-Hydraulic properties

The highest reservoir permeability of 50 mD (1 mD is equal to 10^{-15} m^2) was determined by laboratory experiments on core samples from of the Elbe basis sandstone (Trautwein & Huenges, 2005). (Holl, et al., 2003) confirmed these values by log interpretation. Milsch, et al. (2009) studied the geochemistry of the reservoir fluid under initial pressure, temperature and fluid salt content. He concluded that matrix permeability is not influenced by long term production. A constant permeability of 2 mD (150º C and 45 MPa effective mean stress) was measured. An overview of thermal parameters of the North German basin is given by (Lotz, 2004) and (Gehrke, 2007) which can be summarized in Table 1.

Table 1: Hydrothermal properties.

Geological unit	Permeability [mD]	Porosity [%]	Heat conductivity [kj/(day*m*K)]	Heat Capacity Kj/(m3.K)
Hannover	0.05	1	164.16	2438
Elbe alt.	12.5	3	164.16	2438
Elbe II	25	8	250.56	2438
Elbe I	50	15	241.92	2438
Havel	0.2	0.002	259.2	2650
Volcanic	0.2	0.5	198.72	3657

Mechanical Properties

When a material behaves linear elastically, two elastic moduli characterize its stress- strain behaviour (e.g. Young's modulus and Poison's ratio or λ and μ) however; the constitutive equations in poroelasticity are described by four independent material properties (drained and undrained bulk moduli are also required). The elastic moduli of Rotliegend sandstone were investigated in the laboratory by employing an outcrop rock, equivalent to the reservoir rock (Flechtinger sandstone). Young's modulus, Poison's ratio and unconfined strength of the Flechtinger sandstone were obtained by performing a drained uniaxial test. Young's Modulus and Poisson's ratio were obtained at 50% axial peak stress. The deviation from elastic behaviour (Yield point) was observed to be at 38 MPa. Flechtinger sandstone has a bulk modulus of 15.9 GPa.

Table 2: Mechanical properties of Flechtinger sandstone, an equivalent outcrop to reservoir rock, were measured under drained uniaxial condition.

Poisson's ratio	Young Modulus [GPa]	Peak stress [MPa]	Yield point [MPa]	Tensile Strength* [MPa]
0.31	18	56.7	38	3.9

Not only deformation of Flechtinger sandstone is of interest but also its strength. Hecht, et al., (2005) stated that strength properties mostly depend on the compositional order; however primary rock properties such as density and porosity depend on the grain distribution and the cementation grade of the rock. The tensile strength of the Flechtinger sandstone was measured to be about 3.9 MPa.

Hydro-thermal modeling

The hydro-thermal simulation was carried out using Eclipse 100. This hydrothermal reservoir model led to a total of 60*54*13 grid cells. The model reservoir includes one injection and one production well. In ECLIPSE 100 an energy conservation equation is solved at the end of each converged time step, and the grid block temperatures are updated. The reservoir fluid defined to be pure water and a deterministic approach was employed to populate the reservoir properties. The planned production rate is 20 l/s. The simulation results show that temperature perturbation due to injection does not reach the boundaries of the model. The temperature front propagates through the reservoir, immediately after reinjection of the 70ºC cold water into the reservoir. Fig.5 shows the final temperature field after 30 years of production and injection. Fig.6 shows the transition of the temperature front at different observation points between injection and production wells in the Dethlingen formation. The temperature close to the injection well will drop quite fast to 70ºC. The thermal breakthrough occurs after 30 years of water cycling.

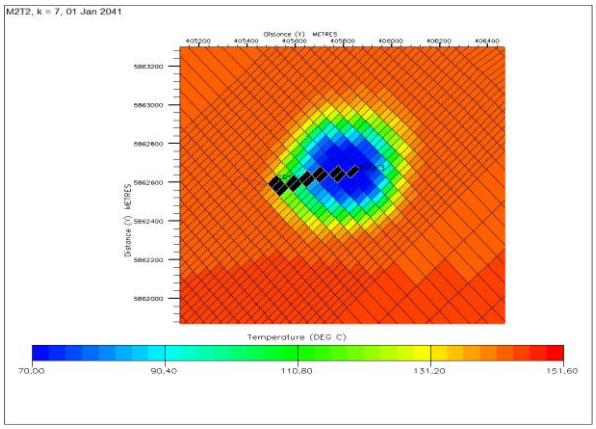

Figure 5: a top view of temperature profile at the end of the simulation. Temperature front develops by diffusion.

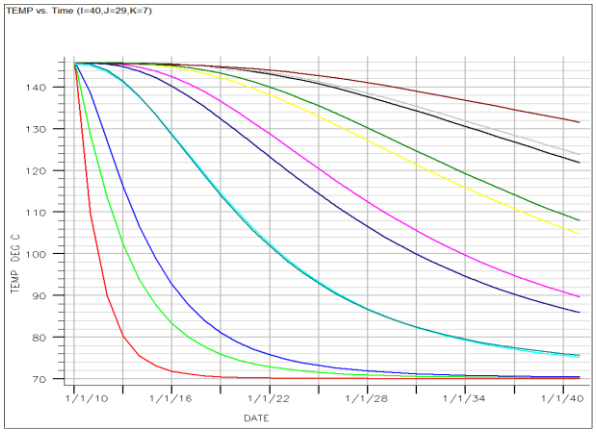

Figure 6: Temperature profile vs. time at observation points shown in Fig.5. Temperature drops relatively fast close to the injection well.

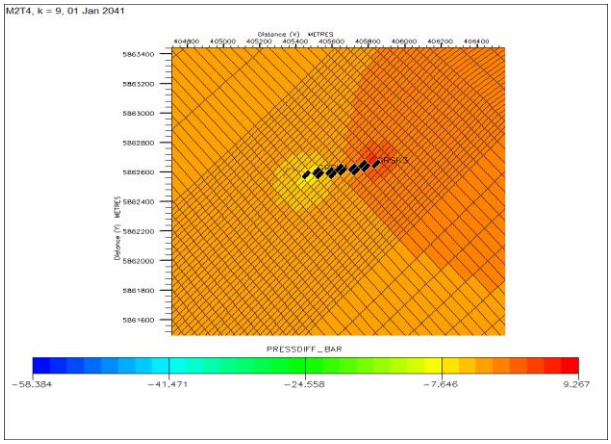

Figure 7: a top view of pressure profile between injection and production well at top of the Deth-Elbe Base sandstone II.

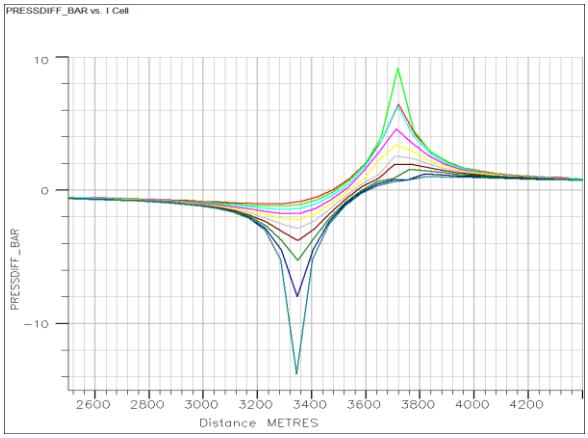

Figure 8: deviation of pressure from equilibrium across the injection and production wells (observation points have been shown in Fig.7).

Thermo-hydro-mechanical coupling

The geomechanics module solves for the force equilibrium of the formation and calculates the displacements (volumetric dilation and compression). There are different approaches to solve and couple the partial differential equations which produce the fluid pressure, temperature and displacement field. For example, in one way coupling the changes in fluid pressure field produce stresses and strains but changes in stress and strain field are assumed not to influence on fluid pressure. Therefore, pressure field can be solved independently of the strain stress field. The same coupling approach can be described for one way thermoelasticity coupling. ECLIPSE™ 100 calculates pore-pressure and temperature distributions which are used in the stress calculations to determine equilibrium levels of effective stress. In Visage™ a staggered scheme is implemented which solves for stresses and updates the hydraulic properties as frequented by user (permeability or porosity). The finite element grid for the stress calculation is the same grid that is used when calculating fluid flow. Compressive stress is negative. The current model solves for the temperature distribution, however does not take into account the thermal stresses. The poroelastic and thermoelastic stresses were estimated based on the laboratory data. An analytical calculation of stress variation is presented in Table 3. A higher pore efficiency of 0.9 is required to make the horizontal minimum stress tensile and higher than strength of the rock.

Table 3: Estimates of stress evolution

Pore Pressure change [MPa]	Bulk modulus [GPa]	Biot coefficient	Poroleastic stress [MPa]	Thermoelastic stress [MPa]	Minimum Horizontal stress [MPa]
0.1	9.3	0.64	-0.35	16.7	-10.2
10	8.6	0.7	-3.85	15.4	-5.7
10	8.6	0.9	-4.95	15.45	3.92

In some cases it is also essential to analyse the geomechanical behaviour outside of the target fluid reservoir. For instance, lateral continuity of the overburden can influence estimates of the ground movement above the reservoir all the way to the surface. In this case, two different grids can be assigned: One which covers the volume of interest with regards to fluid flow and heat transfer (within the reservoir) and one which covers the volume of interest (extended or embedded grids). Poroelastic and thermo-elastic contraction or expansion of the zone from which the fluids are produce or injected changes the shear and normal stress in the reservoir. It also influences where the fluid mass content does not change. The geometry of the geomechanical model including overburden, underburden and sideburden is shown in *Figure 9*. The fluid reservoir considered here is of 3km ×4 km×0.3 km in size which is surrounded by 8 overburden layers on top and 5 underburden layers at the bottom (both 3.7 km). The sideburden layers are extended up to 6 km.

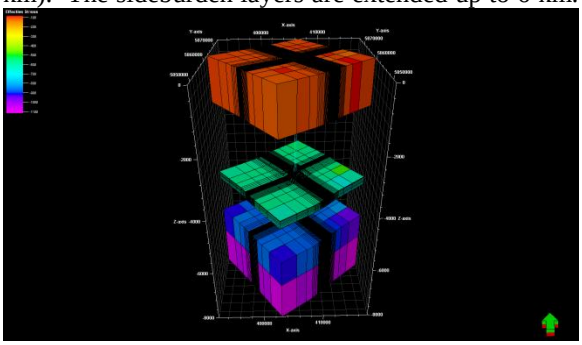

Figure 9: Embedded reservoir model has 66×60×23 cells.

Different boundary condition can be applied to the model. Two different boundary conditions have been specified: 1-Fixed boundary, in which the sides and base of the model are fully fixed in all three directions. 2-Sliding boundary, in which the sides are horizontally fixed, while the base is vertically fixed. The change in vertical effective stress at the cap rock is negligible (*Figure 10*).

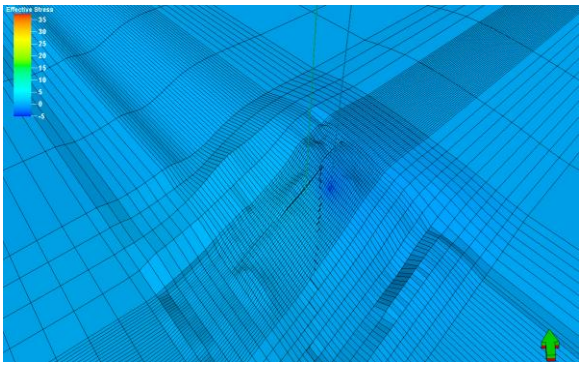

Figure 10: The change of vertical effective stress (bar) at the cap rock due to low porosity is negligible.

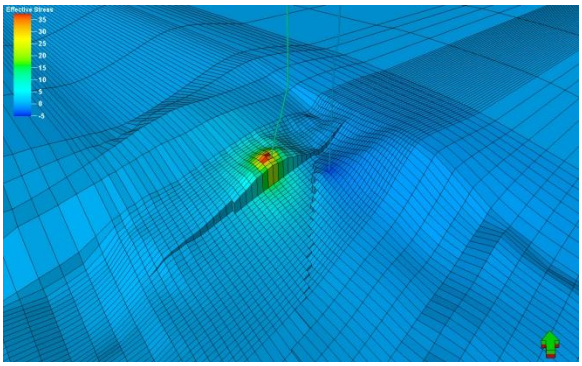

Figure 11: maximum vertical effective stress change (bar) was observed at completion points in the volcanic rock.

The most pronounced stress changes are in the reservoir rock and in the vicinity of production well (*Figure 11*). In the surrounding rock the stress changes are much lower. In contrast, vertical elastic displacement is more pronounced at the most upper layer of the reservoir (*Figure 12*). *Figure 13* shows the vertical displacement at the end of simulation in volcanic layer. The results show a maximum subsidence of 1.75 mm and a maximum uplift of 1.5 mm in the cap rock layer. These values in the volcanic rock are in the order of 0.5 mm (subsidence) mm and 0.05 mm (uplift). At the ground surface the displacement of the rock is in order of micrometres (*Figure 14*).

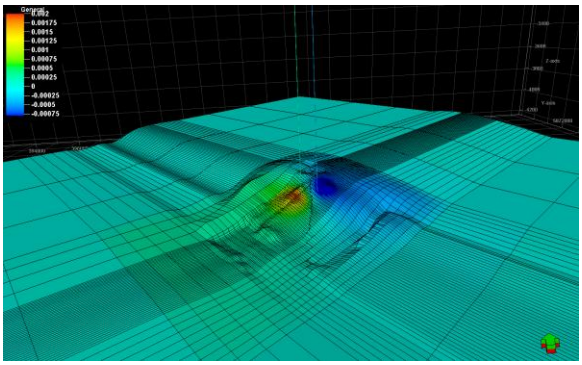

Figure 12: Vertical elastic displacement at the most upper layer of the reservoir (cap rock) at the end of the simulation.

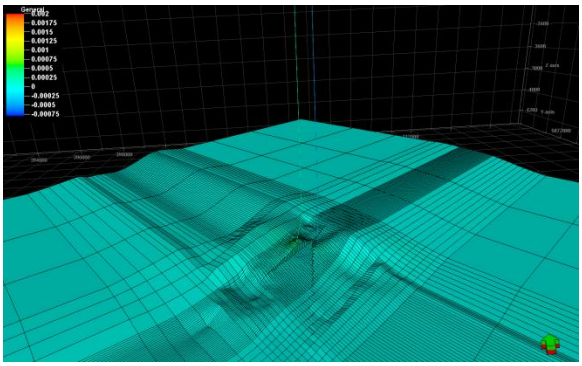

Figure 13: Vertical elastic displacement at the most lowest layer of the reservoir (volcanic rock) at the end of the simulation.

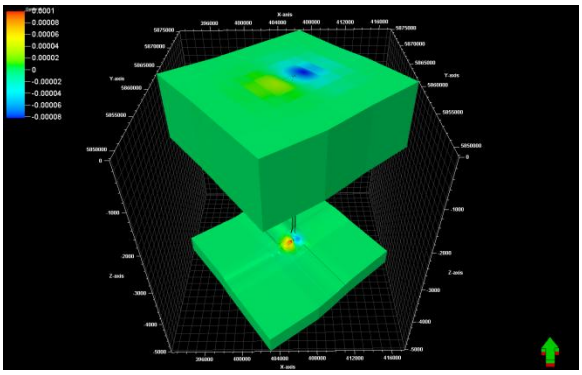

Figure 14: vertical deformation due to injection and production at the surface and below the reservoir (subsidence and uplift)

CONCLUSION

The thermo-hydromechanical modelling of a geothermal reservoir was achieved by employing staggered approach. The results show that effective vertical stress is expected to increase up to 3.5 MPa around the production well. It will decrease 0.5 MPa in the vicinity of injection well. Also a temperature change of 80ºC occurs around the injection well. At this condition a high contribution of pore pressure in

total stress (Biot coefficient) is required to fracture the rock, i.e. a Biot coefficient of 0.9. The maximum vertical effective stress changes takes place close to production well (especially at volcanic rocks), while the highest vertical displacement would occur at the cap rock. The theoretical estimate of thermoelastic stress shows a much higher magnitude in comparison with poroelastic stress.

BIBLIOGRAPHY

Barton, C., Zoback, M., & Moos, D. (1995). "Fluid flow along potentially active faults in crystalline rock". *Geology , 23*(8), 683–686.

Bloecher, G., Zimmermann, G., Moeck, I., Brandt, W., Hassanzadegan, A, et al. (2010). "3D Numerical Modeling of Hydrothermal Processes during the Life-time of a Deep Geothermal Reservoir", *Geofluids, 10*(3), 406-421.

Detournay, E., & Cheng, A. (1988). "Fundamentals of poroelasticity", *In comprehensive rock engineering: pricciples. practice and projects., 2*, 113-171.

Fjaer, E., Holt, R., Horsrud, P., & Raaen, A. M. (1992). "*Petroleum Related Rock Mechanics,*. Amsterdam: Elsevier.

Gehrke, D. (2007). "*Thermisch-hydraulische 3D Modellierung des geothermischen Reservoirs um die Dublette (E GrSk 3/90 / Gt GrSk 4/05) von Groß Schönebeck unter Berücksichtigungvon Stimulationsmaß-nahmen"*, Greifswald: Institut für Geographie und Geologie, Ernst-Moritz-Arndt Universität.

GeoQuest. (2010). *GeoQuest-"Reservoir Simulation Suite"*, Schlumberger.

Hecht, C., Bnsch, C., & Bauch, E. (2005). "Relations of rock structure and composition to petrohysical and geomechanical rock properties: Examples from permocarboniferious red-beds", *Rock mechanics and Rockengineering, 38*(3), 197-216.

Holl, H.-G., Hurter, S., Saadat, A., Köhler, S., Wolfgramm, M., Zimmermann, G., et al. (2003, Sept.). "First hand experience in a second hand borehole", *International Geothermal Conference: Hydraulic experiments and scaling in the geothermal well Groß Schönebeck after reopening*.

Huenges, E., Holl, H.-G., Bruhn, D., Brandt, W., Saadat, A., Moeck, I., et al. (2007). "Current state of the EGS project Groß Schönebeck – drilling into the deep sedimentary geothermal reservoir.", Proceedings European Geothermal Congress

Jaeger, J., Cook, N., & Zimmermann, R. (2007). "*Fundamentals of Rock Mechanics"*, Oxford: Blackwell.

Kwiatek, G., Bohnhoff, M., Dresen, G., Schulze, A., Schulte, T., Zimmermann, G., et al. (2008). "Microseismic event analysis in comjunction with stimulation treatment at the geothermal research well GTGRSK4/05 In Gross Schoenebeck geothermal reservoir", *proceedings, Thirty-third workshop on geothermal reservoir engineering Stanford university, Stanford, California, SGP-TR-185*.

Legarth, B., Huenges, E., & Zimmermann, G. (2005). "Hydraulic fracturing in a sedimentary geothermal reservoir: results and implication", *Int J Rock Mech Mining Sci, 42*, 1028–1041.

Lotz, B. (2004). "*Neubewertung des rezenten WÄarmestroms im Nordostdeutschen Becken"*, FU Berlin: PhD Thesis.

Milsch, H., Seibt, A., & Spangenberg, E. (2009). "Long-term petrophysical investigations on geothermal reservoir rocks at simulated in situ conditions", *Transport in Porous Media, 77*(1), 59-78.

Moeck, I., Schandelmeier, H., & Holl, H. (2008). "The stress regime in a Rotliegend reservoir of the Northeast German Basin", *International Journal of Earth Sciences, 98*(7), 1643-1654.

RGCoE. (2010). *Reservoir Geomechanics Center of Excellence.* Schlumberger .

Segall, P., & Fitzgerald, S. (1998). "A note on induced stress changes in hydrocarbon and geothermal reservoir", *Tectonophysics, 289*, 117-128.

Trautwein, U., & Huenges, E. (2005). "Poroelastic behaviour of physical properties in rotliegend sandstones under uniaxial strain", *International Journal of Rock Mechanics and Mining Sciences, 42*(7-8), 924-932.

Zimmermann, G., Reinicke, A., Blöcher, G., Milsch, H., Gehrke, D., Holl, H.-G., et al. (2007, January 22-24). "Well path design and stimulation treatments at the geothermal research well GTGRSK4/05 In Groß Schönebeck", *thirty-second workshop on geothermal reservoir engineering.* Stanford, California: Stanford University.